Fault-Tolerant Control of Autonomous Surface Vessels Subject to Steer Jamming for Harbor Returning

Bin Liu, Hai-Tao Zhang, *Senior Member, IEEE*, Haofei Meng, and Jun Wang, *Life Fellow, IEEE*

***Abstract*—Steering jam is a common fault of autonomous surface vessels (ASVs) frequently encountered in practical operations. In such a scenario, the allowable ASV moving direction is confined to a narrow zone, which inevitably induces technical challenges for harbor-returning operations of ASVs. As a remedy, we propose a moving-direction fault-tolerant control method for steering jammed ASVs to return to harbors autonomously. We derive sufficient conditions to guarantee the asymptotical stability of the closed-loop ASV system. We elaborate on experimental results on a HUSTER-16 platform established by us to substantiate the effectiveness of the proposed method.**

***Index Terms*—Control systems, fault tolerance, motion control.**

I. Introduction

RECENT decades have witnessed the tremendous advancer of autonomous surface vessels (ASVs), as indispensable tools in ocean engineering. Owing to their high efficiency, broad coverage, superb agility and flexibility, and low running cost, ASVs have been widely deployed for aquatic quality monitoring, marine surveys, reconnaissance, rescue, convoy, and so on. However, in marine operations, the motion of ASVs often suffers from marine environmental interferences such as winds, waves, tides, surges, and obstacles (reefs and mud), which often lead to ASV actuator failures. Consequently, fault-tolerant motion control becomes an essential issue in the research and development of advanced ASVs.

Quite a few efforts have been devoted to the ASV fault-tolerant control (FTC) in recent years. For example, Park and Yoo [1] proposed a performance design methodology for the fault-tolerant tracking of ASVs with unknown faults in nonlinear dynamics and saturated actuators. Fu et al. [2] designed a robust fault-tolerant tracking controller by introducing a radial basis function neural network and an adaptive control protocol into a sliding-mode controller. Afterward, they [3] addressed the trajectory tracking control of ASVs with soft output constraints. Lin et al. [4] proposed an FTC scheme with a fault state observer for the precise positioning of vessels under thruster faults. Zheng et al. [5] developed a robust control method with the assistance of a model-predictive control (MPC) scheme for the trajectory tracking of ASVs suffered from sensor failures. Hu et al. [6] designed a robust adaptive neural-network-based control law for the precise positioning of vessels with input constraints. He et al. [7] and Chen et al. [8] employed neural networks to approximate the unknown external disturbances and uncertain hydrodynamics of ASVs. Cavanini and Lppoliti [9] proposed a fault-tolerant MPC for overactuated vessels. Zheng et al. [10] developed an error-constrained line-of-sight path-following control method for ASVs with system uncertainties, environmental disturbances, and actuator saturations and faults. Wang et al. [11] developed a finite-time passive FTC scheme for the trajectory tracking of ASVs. Zhang et al. [12], [13] proposed fixed-time sliding-mode control protocols for the trajectory tracking of ASVs with system uncertainties, actuator faults, and external disturbances. Singh and Bhushan [14] leveraged a fault classification method nourished by wavelet transforms and support vector machines to improve the steady-state operation of ASVs. Then, Huang et al. [15] proposed an adaptive finite-time FTC protocol for multiple underactuated ASVs with actuator faults, whereas Ghommam and Saad [16] dealt with a leader–follower formation control problem for a fleet of underactuated ASVs with partially known control inputs. Moreover, Peng et al. [17], [18] addressed the event-triggered dynamic surface control of ASVs with unknown kinetics and summarized the applications of fault control for multi-ASV systems, which provides another promising approach for FTC.

Manuscript received 24 May 2022; revised 22 August 2022; accepted 6 October 2022. Date of publication 25 October 2022; date of current version 3 April 2023. This work was supported in part by the National Natural Science Foundation of China under Grant 62225306, Grant U2141235, Grant 62003145, and Grant 61803166, in part by the Research Grants Council of the Hong Kong Special Administrative Region of China under Grant 11202318, and in part by the China Postdoctoral Science Foundation under Grant 2020M672358. *(Corresponding author: Hai-Tao Zhang.)*

Bin Liu is with the School of Artificial Intelligence and Automation and the Key Laboratory of Imaging Processing and Intelligence Control, Huazhong University of Science and Technology, Wuhan 430074, China (e-mail: binliu92@hust.edu.cn).

Hai-Tao Zhang is with the School of Artificial Intelligence and Automation, the State Key Laboratory of Digital Manufacturing Equipment and Technology, and the Key Laboratory of Imaging Processing and Intelligence Control, Huazhong University of Science and Technology, Wuhan 430074, China (e-mail: zht@mail.hust.edu.cn).

Haofei Meng is with the School of Automation, Southeast University, Nanjing 210096, China (e-mail: hfmeng@seu.edu.cn).

Jun Wang is with the Department of Computer Science and the School of Data Science, City University of Hong Kong, Hong Kong (e-mail: jwang.cs@cityu.edu.hk).

Color versions of one or more figures in this article are available at https://doi.org/10.1109/TIE.2022.3215842.

Digital Object Identifier 10.1109/TIE.2022.3215842

In applications, if one side of an ASV catamaran loses power or a steering gear gets stuck, the heading angular will be fixed or confined in a very narrow operational zone. In such a situation, the ASV cannot sail in a straight line but could just make spiral motions. It becomes arduous to perform the navigational trajectory tracking operation, which almost denies the possibility of autonomously harbor returning. Owing to the challenges in control law design, the existing ASV control methods have touched the FTC problem of executor zonal heading jam. Instead, most of the existing relevant FTC laws consider faults such as actuator nonlinearities, input saturations, and so on. In such scenarios, ASVs still could travel in straight lines, which is essentially different from the present FTC scenario where ASVs can just move along spiral curves. In brief, the advantage of the present study lies in proposing a harbor-returning control law for ASVs with executor zonal heading jam faults, which governs ASVs to move along fixed directions by periodically adjusting the forces executed on different sections of the spiral sailing trajectories. Therefore, it becomes an important yet challenging issue to develop niche fault-tolerant trajectory tracking control methods to carry out the autonomous harbor-returning operations for ASVs suffering from monotonous heading faults.

In this article, we propose a periodic-forward control (PFC) to regulate the actuator power according to the positions of the ASV spiral motions, which guarantees the feasibility of heading in any desirable direction. Sufficient conditions are derived based on the Lyapunov theory to ensure the asymptotical stability of the closed-loop ASV system. In brief, the contribution of this study is twofold.

1) A PFC is proposed for ASVs suffering from monotonous heading faults theoretically guaranteed asymptotical stability.
2) The developed PFC is implemented to a 1.6-m-long HUST16 ASV with a rudder angle stuck fault to complete the autonomous harbor-returning task.

The rest of this article is organized as follows. In Section II, the kinematics and dynamics of the ASV are introduced, and thereby, the problem is formulated. Afterward, the PFC is proposed in Section III, and sufficient conditions are derived in Section IV to guarantee the asymptotical stability of the closed-loop ASV system. In Section V, experimental results are elaborated to substantiate the effectiveness of the proposed FTC method. Finally, Section VI concludes this article.

Throughout this article, the following notations are used: $\mathbb{R}$ and $\mathbb{R}^+$ denote the real number and positive real number sets, respectively; $\mathbb{Z}$ and $\mathbb{Z}^+$ denote the integer and positive integer sets, respectively. The function $\arctan(x)$ is an extended arctangent function within a range of $[-\pi, \pi)$. The input saturation function

$$\text{sat}(x) := \begin{cases} \overline{x}, & x > \overline{x}, \\ x, & \underline{x} < x < \overline{x} \\ \underline{x}, & x < \underline{x} \end{cases} \tag{1}$$

with real constants $\overline{x}$ and $\underline{x}$ denoting the predetermined upper and lower bounds of a real variable x, respectively.

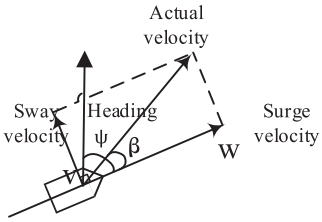

Fig. 1. Illustration of the kinematics of a vessel.

II. Problem Formulation

Consider a three-degree-of-freedom ASV model shown in Fig. 1, whose kinematics is described as

$$\dot{\eta} = \mathbf{R}(\psi)\mathbf{v} \tag{2}$$

where $\boldsymbol{\eta} = [x, y, \psi]^\mathsf{T}$ is the position and heading of the ASV in the Earth-fixed reference frame (EF), $\mathbf{v} = [w, v, r]^\mathsf{T}$ denotes the surge, sway, and yaw velocities of the ASV in a body-fixed reference frame (BF), and $\mathbf{R}(\psi)$ is the rotation transforming matrix from BF to EF

$$\mathbf{R}(\psi) = \begin{bmatrix} \sin(\psi) & -\cos(\psi) & 0 \\ \cos(\psi) & \sin(\psi) & 0 \\ 0 & 0 & 1 \end{bmatrix}.$$

Suppose that the following three assumptions hold [19], [20]: 1) the heave, roll, and pitch modes induced by wave, wind, and current drift forces may be neglected; 2) the inertia, added mass, and hydrodynamic damping matrices are diagonal, which holds for ASVs with port/starboard and fore/aft symmetry; and 3) the ASV is governed by the control signals of the surge force τ_u and yaw moment τ_r. Thus, the ASV dynamics model becomes

$$\begin{aligned} \dot{x} &= w\sin(\psi) - v\cos(\psi) \\ \dot{y} &= w\cos(\psi) + v\sin(\psi) \\ \dot{\psi} &= r \\ \dot{w} &= k_1 w + k_2 vr + k_3\tau_u \\ \dot{v} &= k_4 v + k_5 wr \\ \dot{r} &= k_6 r + k_7\tau_r \end{aligned} \tag{3}$$

with $[x, y]^\mathsf{T}$ and ψ being the position and the moving direction of the ASV, respectively, $k_1 = -\frac{d_1}{m_1}$, $k_2 = \frac{m_2}{m_1}$, $k_3 = \frac{1}{m_1}$, $k_4 = -\frac{d_2}{m_2}$, $k_5 = -\frac{m_1}{m_2}$, $k_6 = -\frac{d_3}{m_3}$, $k_7 = \frac{1}{m_3}$, m_1, m_2, and m_3 are the ASV inertia including added mass effects, d_1, d_2, and d_3 are the hydrodynamic damping coefficients in the surge, sway, and yaw, respectively, $\mathbf{u} = [\tau_u, \tau_r]^\mathsf{T}$ is the control input, τ_u is the actuator power, τ_r is the actuator jetting nozzle angle, and w, v, and r are the nominal forward, sway, and angular velocities, respectively. In general, the moving direction function $\psi(\cdot)$ is invertible.

In operations of ASVs, it is often encountered that the control input of an actuator could not be tuned to exactly zero but keeps either negative or positive only all along. For example, the rudders of the monohulls may be corroded by seawater or entangled by see weeds, which usually causes zonal jams. For another

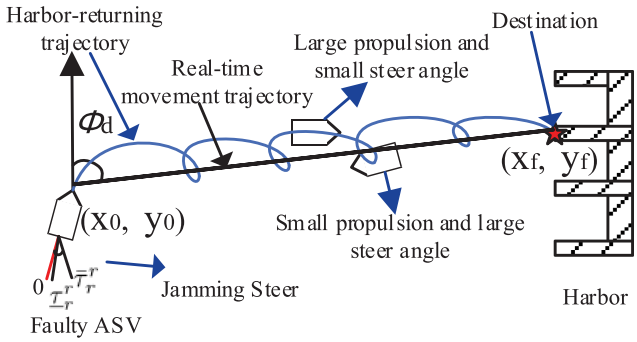

Fig. 2. Illustration of the harbor-returning control, via solving Problem 1.

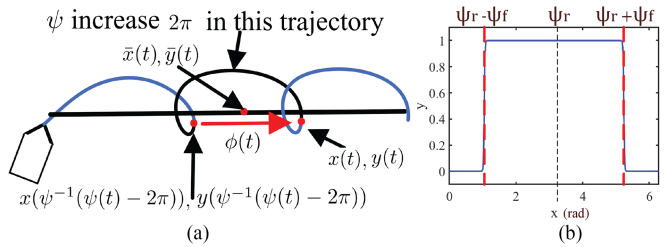

Fig. 3. (a) Illustration of $P(t)$ and $\phi(t)$. (b) Change of function $\varphi(\psi)$ [see (10)] along increasing ψ. Parameters: $k = 0$, $\lambda = 100, \psi_f = 2\pi/3$, and $\psi_r = \pi$.

instance, with mechanical or electrical faults, catamarans might lose power or get stuck on one side. In such a situation, both τ_u and τ_r are confined to very narrow zones excluding zeros, and hence, the ASV could not go along a straight line but just takes some spiral or quasi-spiral motion. Specifically, the actuator stuck saturations are described as

$$\tau_u = \text{sat}\left(\tau_u^r\right), \quad \tau_r = \text{sat}\left(\tau_r^r\right) \tag{4}$$

with actuator power thresholds $\overline{\tau}_u^r, \underline{\tau}_u^r \geq 0$ and jetting nozzle angle thresholds $\overline{\tau}_r^r, \underline{\tau}_r^r > 0$. It immediately follows from (3) that the ASV angular velocity $r(t) > 0, t \in [0, \infty]$ for $r(0) = 0$, implying that the ASV heading ψ increases monotonically, and hence, its dynamics becomes difficulty to be stabilized.

Since the ASV heading $\psi(t)$ increases monotonically, the ASV will move forward along a spiral curve instead with an angular period of 2π. The main problem of the present study is to develop an FTC law for system (3) with actuator stuck saturations (4) to govern the ASV to a predetermined target (i.e., harbor) point $P_f := [x_f, y_f]$, i.e., a harbor pile, as shown in Fig. 2.

Problem 1 (Autonomous harbor-returning control of an ASV with a rudder-stuck fault): Given an ASV with kinetics and dynamics described in (2) and (3), respectively, define a real-time movement position $P(t)$ of the ASV as

$$\begin{aligned} P(t) &:= [\overline{x}(t), \overline{y}(t)]^{\mathsf{T}} \\ \overline{x}(t) &:= \frac{1}{t - \psi^{-1}(\psi(t) - 2\pi)} \int_{\psi^{-1}(\psi(t)-2\pi)}^{t} x(s)ds \\ \overline{y}(t) &:= \frac{1}{t - \psi^{-1}(\psi(t) - 2\pi)} \int_{\psi^{-1}(\psi(t)-2\pi)}^{t} y(s)ds. \end{aligned} \tag{5}$$

Design a position regulation law $\mathbf{u} = [\tau_u, \tau_r]^{\mathsf{T}} = f(x, y, \psi)$ subject to actuator stuck saturation (4), such that

$$\lim_{t \to \infty} P_f - P(t) = \mathbf{0}. \tag{6}$$

III. Harbor-Returning Controller Design

As shown in Fig. 3, to finely tune the moving direction ψ during a spiral ASV motion, we divide the range of ψ into two zones: an angular-tuning zone $\Psi_t := [2k\pi + \psi_r - \psi_f, 2k\pi + \psi_r + \psi_f)$ and an acceleration zone $\Psi_a := [2k\pi + \psi_r + \psi_f, (2k + 2)\pi + \psi_r - \psi_f)$ with $k \in \mathbb{Z}^+$ and $\psi_r \in [0, 2\pi), \psi_f \in [0, \pi)$. Specifically, in the angular-tuning zone, the ASV reduces its forward speed while increasing the steering angular speed, and the reverse in the acceleration zone. Note that the variable ψ_r is used to tune the movement direction ψ for the ASV, which could be adjusted online. ψ_f determines the sizes of the angular-tuning zone Ψ_t and the acceleration zone Ψ_a during a 2π period. Therefore, the constant parameter ψ_f is designed according to the dynamics of the ASV.

Before designing the harbor-returning controller, it is necessary to define a real-time movement direction $\phi(t)$ for the ASV as

$$\phi(t) := \arctan \frac{x(t) - x\left(\psi^{-1}(\psi(t) - 2\pi)\right)}{y(t) - y\left(\psi^{-1}(\psi(t) - 2\pi)\right)}. \tag{7}$$

A continuous periodical quasi-sigmoid function $\varphi(\psi)$ is given as follows:

$$\varphi(\psi) = \frac{1}{1 + \exp(-\lambda f_\varphi(\psi, \psi_r, \psi_f))} \tag{8}$$

where $\lambda > 0$, $f_\varphi(\psi, \psi_r, \psi_f) = f_\varphi(\psi + \delta_\psi, \psi_r + \delta_\psi, \psi_f)$, and $\delta_\psi > 0$ is a period constant. Since $f_\varphi(\cdot)$ is designed such that $f_\varphi(\psi, \psi_r, \psi_f) \geq 0$ for $\psi \in \Psi_a$, and $f_\varphi(\psi, \psi_r, \psi_f) < 0$ elsewise, one has $\varphi(\psi) \to 0$ for $\psi \in [2k\pi + \psi_r - \psi_f, 2k\pi + \psi_r + \psi_f)$, and $\varphi(\psi) \to 1$ for $\psi \in [2k\pi + \psi_r + \psi_f, (2k + 2)\pi + \psi_r - \psi_f)$. Moreover, $\varphi(\psi)$ is a periodical signal with

$$\varphi(\psi) = \varphi(\psi + 2k\pi), \quad k \in \mathbb{Z}. \tag{9}$$

As shown in Fig. 3, ψ_r and ψ_f are tuned according to ASV dynamics (3) and input constraints (4).

Remark 1: Usual sigmoid functions are symmetric and aperiodic, which are not suitable for the present controller design. Therefore, we use a quasi-sigmoid function instead, which is asymmetric with a period of 2π. Without loss of generality, one may use a quasi-sigmoid function

$$\varphi(\psi) = \frac{1}{1 + \exp(-\lambda(\cos(\psi - \psi_r) - \cos(\psi_f)))} \tag{10}$$

with $\lambda > 0$. One may pick other quasi-sigmoid functions for control law design according to specific requirements of different scenarios.

Remark 2: With the zonal jamming fault, the ASV cannot be run in straight lines but just spiral curves, which makes it difficult to directly achieve an effective control law with the

actual heading angle and position of the ASV as the control objective. In order to govern the ASV to a desirable direction to return to the harbor, we propose a spiral forward strategy to regulate the center of the spiral curves to the harbor. Therefore, we introduce φ to divide the periodic angle of 2π into two zones, i.e., an angular-tuning zone and an acceleration zone. More importantly, the average heading $\phi(t)$ of the ASV during this period is controllable, whereas the actual heading not. Therefore, in order to realize the ASV harbor-returning task, it makes more sense to take $\phi(t)$ as the control target.

Now, a fault-tolerant ASV control law is defined as

$$\begin{aligned}\tau_u &= \varphi(\underline{\tau}_u - \overline{\tau}_u) + \overline{\tau}_u \\ \tau_r &= \varphi(\overline{\tau}_r - \underline{\tau}_r) + \underline{\tau}_r \end{aligned} \tag{11}$$

where the thresholds $\underline{\tau}_u, \overline{\tau}_u, \underline{\tau}_r$, and $\overline{\tau}_r$ are determined according to the constraints (4) of the rudder and propeller jamming.

IV. Main Technical Result

Before presenting the main technical result, it is necessary to give a lemma first.

Lemma 1: Given an ASV governed by (2), (3), and an FTC law (8), (11), $\phi(t)$ exponentially converges to $\overline{\phi}(\lambda, \psi_r, \psi_f)$, where $\overline{\phi}(\lambda, \psi_r, \psi_f) \in [0, 2\pi)$ is a constant independent of the initial state $[x(0), y(0), \psi(0)]^{\mathsf{T}}$.

Proof: Since $r(t) > 0$, there exists $T_r(t)$ such that

$$\int_t^{t+T_r(t)} r(s)ds = 2\pi, \quad t > 0. \tag{12}$$

Let $e_r := r(t + T_r(t)) - r(t)$; it follows from (12) that $r(t + T_r(t))(1 + \dot{T}_r(t)) - r(t) = 0$, and $\dot{T}_r(t) = \frac{r(t)}{r(t+T_r(t))} - 1$, which implies that

$$\begin{aligned}&\dot{r}(t + T_r(t)) \\ &= \frac{\partial r(t + T_r(t))}{\partial(t + T_r(t))} \frac{\partial t + T_r(t)}{\partial t} \\ &= \left(1 + \dot{T}_r(t)\right) \dot{r}(t + T_r(t)) \\ &= \left(\frac{r(t)}{r(t + T_r(t))}\right) \dot{r}(t + T_r(t)) \\ &= \left(\frac{r(t)}{r(t + T_r(t))}\right) (k_6 r(t + T_r(t)) + k_7\tau_r(t + T_r(t))) \\ &= k_6 r(t) + \frac{k_7\tau_r(t + T_r(t))r(t)}{r(t + T_r(t))}.\end{aligned}$$

According to (8), one has $\varphi(\psi(t)) = \varphi(\psi(t) + 2\pi) = \varphi(\psi(t + T_r(t)))$, and hence, $\tau_r(t) = \tau_r(t + T_r(t))$, which immediately leads to

$$\begin{aligned}&\dot{r}(t + T_r(t)) - \dot{r} \\ &= k_6 r(t) + \frac{k_7\tau_r(t + T_r(t))r(t)}{r(t + T_r(t))} - \dot{r} \\ &= \frac{r(t)}{r(t + T_r(t))} k_7\tau_r(t + T_r(t)) - k_7\tau_r(t) \\ &= k_7\tau_r(t)\left(\frac{r(t)}{r(t + T_r(t))} - 1\right) \\ &= \frac{k_7\tau_r(t)}{r(t + T_r(t))}(r(t) - r(t + T_r(t)))\end{aligned}$$

and

$$\dot{e}_r = -\frac{k_7\tau_r(t)}{r(t + T_r(t))} e_r.$$

As $k_7 > 0, \tau_r(t) > 0, r(t + T_r(t)) > 0$, and $\tau_r(t), r(t + T_r(t))$ are bounded, there exists a constant k_T such that $0 < k_T < \frac{k_7\tau_r(t)}{r(t+T_r(t))}$. Therefore, $e_r(t)$ exponentially converges to 0.

As $r(t + T_r(t))$ exponentially converges to $r(t)$, one has $\lim_{t\to\infty} \dot{T}_r(t) = \frac{r(t)}{r(t+T_r(t))} - 1 = 0$, and $T_r(t)$ exponentially converges to t_r, where t_r is a constant. Then, let $e_w := w(t + t_r) - w(t)$, $e_v := v(t + t_r) - v(t)$. One has

$$\begin{aligned}\dot{e}_w &= k_1 w(t + t_r) + k_2 v(t + t_r) r(t + t_r) \\ &\quad + k_3\tau_u(t + t_r) - (k_1 w(t) + k_2 v(t) r(t) + k_3\tau_u(t)) \\ &= k_1 e_w + k_2(v(t + t_r) r(t + t_r) - v(t) r(t)) \\ &\quad + k_3(\tau_u(t + t_r) - \tau_u(t)) \\ &= k_1 e_w + k_2 r(t + t_r) e_v + \bar{e}_w \\ \dot{e}_v &= k_4 v(t + t_r) + k_5 w(t + t_r) r(t + t_r) \\ &\quad - (k_4 v(t) + k_5 w(t) r(t)) \\ &= k_4 e_v + k_5(w(t + t_r) r(t + t_r) - w(t) r(t)) \\ &= k_4 e_v + k_5 r(t + t_r) e_w + \bar{e}_v\end{aligned}$$

with $\bar{e}_w := k_2 v(t)(r(t + t_r) - r(t)) + k_3(\tau_u(t + t_r) - \tau_u(t))$ and $\bar{e}_v := k_4 w(t)(r(t + t_r) - r(t))$.

Analogously, since $\lim_{t\to\infty} r(t) = r(t + t_r)$ and $w(t)$ and $v(t)$ are bounded, one has that $\bar{e}_w(t)$ and $\bar{e}_v(t)$ exponentially converge to 0. Let $\mu := [e_w, e_v]^{\mathsf{T}}$; then, one has

$$\dot{\mu} = A\mu + E_\mu \tag{13}$$

with

$$A = \begin{bmatrix} k_1 & k_2 r(t + t_r) \\ k_5 r(t + t_r) & k_4 \end{bmatrix}, \quad E_\mu = \begin{bmatrix} \bar{e}_w \\ \bar{e}_v \end{bmatrix}.$$

Because $k_1 < 0, k_2 > 0, k_4 < 0, k_5 < 0, r(t + t_r) > 0$, A is Hurwitz, and $\lim_{t\to\infty} \dot{\mu} = [0, 0]^{\mathsf{T}}$, $w(t + t_r)$ exponentially converges to $w(t)$ and $v(t + t_r)$ exponentially converges to $v(t)$.

Let $v_x := \dot{x}$, $v_y := \dot{y}$, $e_{vx} = v_x(t + t_r) - v_x(t)$, and $e_{vy} = v_y(t + t_r) - v_y(t)$,

$$\begin{aligned}e_{vx} &= w(t + t_r)\sin(\psi(t + t_r)) - v(t + t_r)\cos(\psi(t + t_r)) \\ &\quad - w(t)\sin(\psi(t)) + v(t)\cos(\psi(t)), \\ e_{vy} &= w(t + t_r)\cos(\psi(t + t_r)) + v(t + t_r)\sin(\psi(t + t_r)) \\ &\quad - w(t)\cos(\psi(t)) - v(t)\sin(\psi(t)).\end{aligned}$$

As $\lim_{t\to\infty} w(t) = w(t + t_r)$, $\lim_{t\to\infty} v(t) = v(t + t_r)$ and $\lim_{t\to\infty} \psi(t) = \psi(t + t_r) - 2\pi$, one has that $\lim_{t\to\infty} e_{vx}(t) = 0$ and $\lim_{t\to\infty} e_{vy}(t) = 0$. Then, let $x_e(t) := x(t + t_r) - x(t), y_e(t) := y(t + t_r) - y(t)$; then, one has that

$\dot{x}_e = v_x(t+t_r) - v_x(t) = e_{vx}$, $\dot{y}_e = v_y(t+t_r) - v_y(t) = e_{vy}$, and $\lim_{t\to\infty} \dot{x}_e(t) = 0$ and $\lim_{t\to\infty} \dot{x}_e(t) = 0$, which immediately leads to the fact that $x_e(t)$ exponentially converges to x_{e0} and $y_e(t)$ exponentially converges to y_{e0}, where x_{e0} and y_{e0} are constants

$$\begin{aligned}
&\lim_{t\to\infty} \phi(t) \\
&= \lim_{t\to\infty} \arctan \frac{x(t) - x(\psi^{-1}(\psi(t) - 2\pi))}{y(t) - y(\psi^{-1}(\psi(t) - 2\pi))} \\
&= \lim_{t\to\infty} \arctan \frac{x_e(t)}{y_e(t)} \\
&= \arctan \frac{x_{e0}}{y_{e0}} \\
&= \overline{\phi}(\lambda, \psi_r, \psi_f)
\end{aligned}$$

with $\overline{\phi}(\lambda, \psi_r, \psi_f) \in [0, 2\pi)$ being a constant. Note that the dynamic of r is linear, so the convergence value $r(\infty)$ is independent of the initial state $[x(0), y(0), \psi(0)]^{\mathsf{T}}$. Since $\begin{bmatrix} k_1 & k_2 r(t) \\ k_5 r(t) & k_4 \end{bmatrix}$ is a Hurwitz, both $w(\infty)$ and $v(\infty)$ are independent of the initial state $[x(0), y(0), \psi(0)]^{\mathsf{T}}$, and both $v_x(t)$ and $v_y(t)$ are independent of the initial state. Accordingly, $\overline{\phi}(\lambda, \psi_r, \psi_f)$ is independent of the initial state either. The proof is, thus, completed.

By alleviating the conditions of Lemma 1 by letting ψ_r be an arbitrary constant in $[0, 2\pi]$, one has the following corollary.

Corollary 1: Given an ASV governed by (2), (3) and control law (8), (11) with constant parameters λ and ψ_f, and $\lim_{t\to\infty} \phi(t, \psi_r) = \overline{\phi}$,

$$\overline{\phi}(\lambda, \psi_r + \Delta\psi, \psi_f) = \overline{\phi}(\lambda, \psi_r, \psi_f) + \Delta\psi$$

with $\Delta\psi \in [0, 2\pi]$.

Proof: As $f_\varphi(\psi, \psi_r, \psi_f) = f_\varphi(\psi + \delta_\psi, \psi_r + \delta_\psi, \psi_f)$ in (8), one has that $\varphi(\psi, \psi_r, \psi_f) = \varphi(\psi + \delta_\psi, \psi_r + \delta_\psi, \psi_f)$. Let $\psi_c = \psi_r + \Delta\psi$; then, one has $\tau_u(\psi(t), \psi_r) = \tau_u(\psi(t) + \Delta\psi, \psi_c)$ and $\tau_r(\psi(t), \psi_r) = \tau_r(\psi(t) + \Delta\psi, \psi_c)$. Moreover, the convergence value $\overline{\phi}$ is independent of the initial state. By rotating the coordinates by an angle $\Delta\psi$, one has $\tau_u(\psi(t), \psi_r) = \tau_u(\psi(t) + \Delta\psi, \psi_r + \Delta\psi) = \tau'_u(\psi'(t), \psi'_r)$ and $\tau_r(\psi(t), \psi_r) = \tau_r(\psi(t) + \Delta\psi, \psi_r + \Delta\psi) = \tau'_r(\psi'(t), \psi'_r)$, which implies that the closed-loop ASV governed by dynamics (2), (3) and control law (8), (11) will reach the same stable state after the coordinate rotational transformation. It can, thus, be derived that $\lim_{t\to\infty} \phi'(t) = \overline{\phi}$ and $\lim_{t\to\infty} \phi(\psi_r + \Delta\psi) = \overline{\phi}(\psi_r + \Delta\psi) = \lim_{t\to\infty} \phi'(t) + \Delta\psi = \overline{\phi} + \Delta\psi$, and the proof is completed.

It is proved in Corollary 1 that if ψ_r varies by an angle $\Delta\psi$, then the eventual value $\overline{\phi}$ varies by the same angle $\Delta\psi$ as well. Therefore, there exists a constant $\psi_s > 0$ such that, for any constant ψ_r, one has $\overline{\phi} = \psi_r + \psi_s$, where ψ_s can be tuned via numerical simulation.

As $\phi(t)$ is continuous and differentiable, according to Lagrange's mean-value theorem, there exists a continuous function $f(\phi, \psi_r + \psi_s)$ such that

$$\dot{\phi} = f(\phi, \psi_r + \psi_s) + \psi_r + \psi_s - \phi. \tag{14}$$

Given a control target $\phi_d(t)$, let $\phi_e = \phi - \phi_d$; then, one has

$$\dot{\phi}_e = f(\phi, \psi_r + \psi_s) + \psi_r + \psi_s - \phi - \dot{\phi}_d. \tag{15}$$

Once $\dot{\phi}_d = 0$, design $\psi_r = \phi_d - \psi_s$; then, one has

$$\begin{aligned}
\dot{\phi}_e &= f(\phi, \phi_d) + \phi_d - \phi \\
&= f(\phi, \phi_d) - \phi_e.
\end{aligned}$$

It thus follows from Lemma 1 and Corollary 1 that

$$\lim_{t\to\infty} \phi = \phi_d.$$

By the inverse Lyapunov theorem [21], there exists a Lyapunov function $V_\phi(\phi_e)$ and constants $c_1, c_2, c_3 > 0$ such that the following inequalities hold:

$$\begin{aligned}
c_1\|\phi_e\|^2 \quad &\le \quad V_\phi(\phi_e) \le c_2\|\phi_e\|^2 \\
\frac{\partial V_\phi}{\partial \phi_e}(f(\phi, \phi_d) + \phi_d - \phi) &\le -c_3\|\phi_e\|^2.
\end{aligned} \tag{16}$$

When $\dot{\phi}_d \neq 0$, a control law is defined as

$$\begin{aligned}
\dot{\xi} &= -\alpha_1\phi_e + \ddot{\phi}_d \\
\psi_r &= \phi + \xi - \alpha_2\phi_e - \psi_s
\end{aligned} \tag{17}$$

where $\alpha_1 > 0$, $\alpha_2 > 0$, and ξ is an intermediate state variable.

Then, we have the following result.

Lemma 2: Given an ASV governed by (2), (3) and control protocol (8), (11), (17), if there exist positive parameters α_1 and α_2 such that

$$|(c_3 + \alpha_2 - 1)\phi_e| > \max|f(\phi, \phi + \xi - \alpha_2\phi_e) - f(\phi, \phi_d)| \tag{18}$$

with $\phi_e \neq 0$, then $\lim_{t\to\infty} \phi = \phi_d$.

Proof: Let $\widetilde{\xi} = \xi - \dot{\phi}_d$; then, by (2), (3), (8), (11), and (17), the closed-loop ASV system can be rewritten as

$$\begin{aligned}
\dot{\widetilde{\xi}} &= -\alpha_1\phi_e \\
\dot{\phi}_e &= f(\phi, \psi_r + \psi_s) + \widetilde{\xi} - \alpha_2\phi_e.
\end{aligned} \tag{19}$$

Let a Lyapunov function candidate be $V_\xi = \frac{1}{2\alpha_1}\widetilde{\xi}^2 + \frac{1}{2}V_\phi$ with $V_\phi = \|\phi_e\|^2$; then, one has

$$\begin{aligned}
&\dot{V}_\xi \\
&= \widetilde{\xi}\dot{\widetilde{\xi}} + \frac{\partial V_\phi}{2\partial \phi_e}(f(\phi, \psi_r + \psi_s) + \widetilde{\xi} - \alpha_2\phi_e) \\
&= -\widetilde{\xi}\phi_e + \frac{\partial V_\phi}{2\partial \phi_e}(f(\phi, \psi_r + \psi_s) + \widetilde{\xi} - \alpha_2\phi_e) \\
&= -\widetilde{\xi}\phi_e + f(\phi, \psi_r + \psi_s)\phi_e + \widetilde{\xi}\phi_e - \alpha_2\phi_e^2 \\
&= f(\phi, \psi_r + \psi_s)\phi_e - \alpha_2\phi_e^2 \\
&= (f(\phi, \psi_r + \psi_s) - f(\phi, \phi_d))\phi_e - (\alpha_2 - 1)\phi_e^2 \\
&\quad + f(\phi, \phi_d)\phi_e - \phi_e^2 \\
&= (f(\phi, \psi_r + \psi_s) - f(\phi, \phi_d))\phi_e - (\alpha_2 - 1)\phi_e^2 \\
&\quad + \frac{\partial V_\phi}{\partial \phi_e}(f(\phi, \phi_d) + \phi_d - \phi)
\end{aligned}$$

$$\leq (f(\phi,\psi_r+\psi_s)-f(\phi,\phi_d))\phi_e-(\alpha_2-1)\phi_e^2-c_3\|\phi_e\|^2$$
$$\leq (f(\phi,\psi_r+\psi_s)-f(\phi,\phi_d))\phi_e-(c_3+\alpha_2-1)\phi_e^2.$$

By virtue of (18), it could be derived that

$$\begin{aligned}\dot{V}_\xi &\leq (f(\phi,\psi_r+\psi_s)-f(\phi,\phi_d))\phi_e-(c_3+\alpha_2-1)\phi_e^2\\ &\leq (c_3+\alpha_2-1)\phi_e^2-(c_3+\alpha_2-1)\phi_e^2\\ &\leq 0\end{aligned}$$

where $\dot{V}_\xi=0$ if and only if $\phi_e=0$. Therefore, $\lim_{t\to\infty}\phi_e=0$ and $\lim_{t\to\infty}\phi=\phi_d$ with the LaSalle invariance principle [21]. The proof is, thus, completed.

Now, we are ready to give the main technical result.

Theorem 1: Given an ASV with dynamics (2), (3), let the destination harbor heading $\phi_d:=\arctan(\frac{x_f-\overline{x}}{y_f-\overline{y}})$; under (18), one has that Problem 1 is solved by control law (8), (11), (17).

Proof: Define the tangential direction of the real-time movement trajectory in $P(t)$ as $\phi_p(P(t))$. One has

$$\begin{aligned}&\lim_{\delta\to0}\phi_p(P(t+\delta)-P(t))\\ &=\lim_{\delta\to0}\arctan\left(\frac{\overline{x}(t+\delta)-\overline{x}(t)}{\overline{y}(t+\delta)-\overline{y}(t)}\right)\\ &=\lim_{\delta\to0}\arctan\left(\frac{\int_{\psi^{-1}(\psi(t)-2\pi)+\delta}^{t+\delta}x(s)ds-\int_{\psi^{-1}(\psi(t)-2\pi)}^{t}x(s)ds}{\int_{\psi^{-1}(\psi(t)-2\pi)+\delta}^{t+\Delta t}y(s)ds-\int_{\psi^{-1}(\psi(t)-2\pi)}^{t}y(s)ds}\right)\\ &=\lim_{\delta\to0}\arctan\left(\frac{\int_t^{t+\delta}x(s)ds-\int_{\psi^{-1}(\psi(t)-2\pi)}^{\psi^{-1}(\psi(t)-2\pi)+\delta}x(s)ds}{\int_t^{t+\delta}y(s)ds-\int_{\psi^{-1}(\psi(t)-2\pi)}^{\psi^{-1}(\psi(t)-2\pi)+\delta}y(s)ds}\right)\\ &=\lim_{\delta\to0}\arctan\left(\frac{x(t)-x(\psi^{-1}(\psi(t)-2\pi))}{y(t)-y(\psi^{-1}(\psi(t)-2\pi))}\right)\\ &=\phi(t)\end{aligned}$$

which implies that

$$\dot{P}(t)=[\nu(t)\sin(\phi(t)),\nu(t)\cos(\phi(t))]^{\mathsf{T}} \tag{20}$$

with $\nu(t)\geq0$.

By Lemma 2, with the control law (8), (11), (17), one has that $\lim_{t\to\infty}\phi=\phi_d$. Then, let $l_p(t):=\|P_f-P(t)\|$. One has

$$\begin{aligned}\dot{l}_p(t)&=\nu(t)\cos\left(\pi-(\phi-\phi_p(P_f-P(t)))\right)\\ &=-\nu(t)\cos\left(\phi-\phi_d\right).\end{aligned}$$

Let $V_p=\frac{1}{2}\|l_p\|^2$ and $e_p=1-\cos(\phi-\phi_d)$; then, one has

$$\begin{aligned}\dot{V}_p&=l_p\dot{l}_p\\ &=-l_p\nu(t)\cos(\phi-\phi_d).\end{aligned}$$

Since $\lim_{t\to\infty}\phi=\phi_d$, there exists $T_p>0$ such that $|\phi-\phi_d|<\frac{\pi}{2}, t>T_p$. Let $V_{p1}=-\int_0^{T_p}l_p(s)\nu(s)\cos(\phi(s)-\phi_d(s))ds$ and $V_{p2}=-\int_{T_p}^{t}l_p(s)\nu(s)\cos(\phi(s)-\phi_d(s))ds$; then, one has that $V_{p2}<0$, and there exists a finite $N_p>0$ such that $V_{p1}<N_p$ due to the limitation of input constraints. Therefore, $V_p=V_{p1}+V_{p2}$ is upper bounded, and $\lim_{t\to\infty}l_p\nu=0$ by Barbalat's lemma [21]. If $\lim_{t\to\infty}\nu=0$ and $\lim_{t\to\infty}l_p>0$, one has that $\lim_{t\to\infty}(x(t)-x(\psi^{-1}(\psi(t)-2\pi)))=0$, $\lim_{t\to\infty}(y(t)-y(\psi^{-1}(\psi(t)-2\pi)))=0$, and $\lim_{t\to\infty}(\psi-\psi_0)\neq0$, which contradicts the previous convergence condition. Therefore, if $\lim_{t\to\infty}\nu=0$, one has $\lim_{t\to\infty}l_p=0$. Therefore, $\lim_{t\to\infty}\|P_f-P(t)\|=\lim_{t\to\infty}l_p=0$, and Problem 1 is, thus, solved.

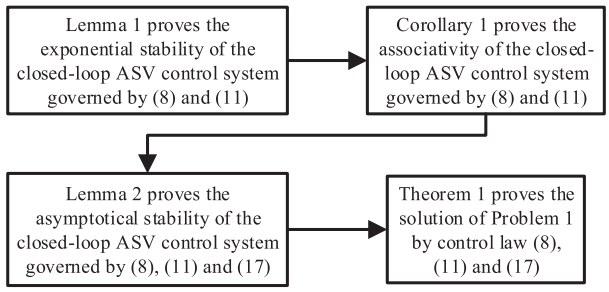

Fig. 4. Logical relationship between the conclusions.

Algorithm 1: Autonomous Fault-Tolerant Harbor-Returning Control Algorithm.

Step 1: Pick parameters ψ_f and ψ_r according to the constraints (4) of the steer jamming, and set k to a non-negative integer;
Step 2: For $k=0:\infty$;
Step 3: Feed the controller signal (10), (11), (17) to an ASV (3);
Step 4: If $|P_f-P(t)|<\epsilon$;
Step 5: Stop and break (harbor-returning finished);
Step 6: End;
Step 7: End;

Combining the above lemmas, corollaries, and theorems, the stability and effectiveness of the harbor-returning controller are proved theoretically. The logical relationship between the conclusions can be expressed in Fig. 4.

To facilitate real control applications of ASVs, the FTC algorithm determined by (8), (11), and (17) is given by Algorithm 1 with an acceptable tolerated error ϵ.

V. Experiments

The experiments are based on our developed 1.6-m-long HUSTER-16 ASV, as shown in Fig. 5. The experimental platform is composed of a Beidou positioning module, an SL-300A motor driver, a 3-kW WJ064 water-jet propeller (composed of a propeller body, a reversing bucket, a jetting nozzle with a $[-20^\circ,20^\circ]$ tuneable jet nozzle angle range, and a motor), an MC02 real-time embedded controller, a wireless LAN hub, and an ABS plastic hull. By zigzag tracking experiments, the dynamics of the ASV is identified as in [22]

$$\begin{aligned}\dot{\psi}&=r\\ \dot{w}&=-1.2235\,w+0.95vr+0.00122\tau_u\\ \dot{v}&=-1.437v-0.105wr\\ \dot{r}&=-1.399r+0.043\tau_r.\end{aligned} \tag{21}$$

Fig. 5. HUSTER-16 ASV platform used in autonomous harbor-returning experiments.

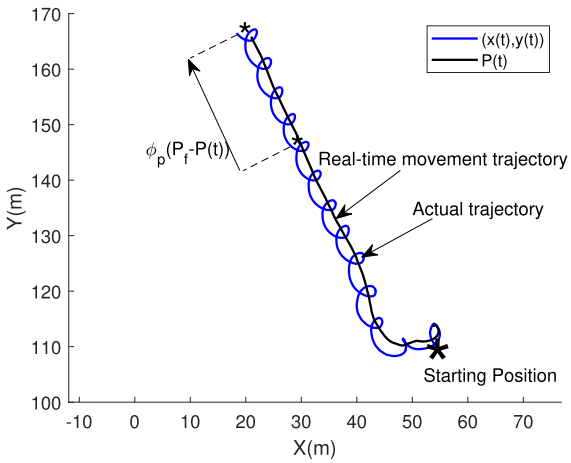

Fig. 6. Experimental trajectory of the closed-loop ASV system governed by (2), (3), and control protocol (8), (11), (17).

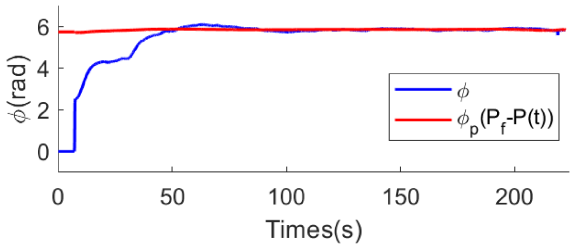

Fig. 7. Temporal behavior of ϕ and $\phi_p(P_f - P(t))$.

The parameters of the control law (10), (11), (17) are set as $\lambda = 100$, $\psi_f = 60°$, $\alpha_1 = 0.35$, $\alpha_2 = 1$, the target position $P_f = [21, 165]^{\mathsf{T}}$, and sampling period $T_s = 0.1$ s. The actuator saturations are picked as $\underline{\tau}_r = 2°$, $\overline{\tau}_r = 18°$, $\underline{\tau}_u = 1000$ r/min, and $\overline{\tau}_u = 4000$ r/min.

The initial position $[x_0, y_0]^{\mathsf{T}} = [56, 109]^{\mathsf{T}}$ m and initial direction $\psi(0) = 5.7336$ rad. The motion trajectory of the ASV illustrated in Fig. 6 fulfills the autonomous harbor-returning task for the ASV with steer jamming fault in Songshan Lake, Guangdong, China. In the experiment, the control period is

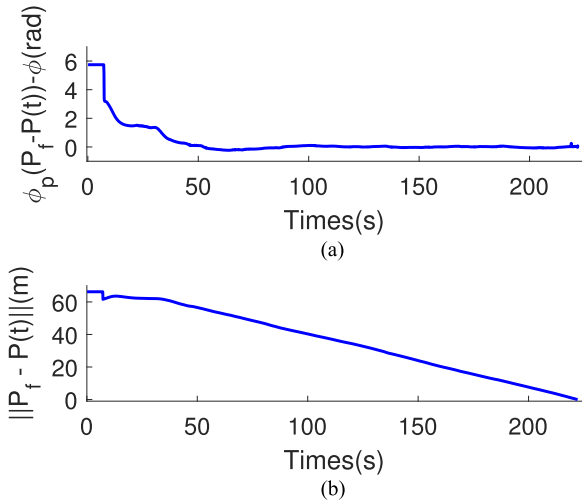

Fig. 8. Temporal behaviors of (a) the ASV harbor-heading error $\phi_p(P_f - P(t)) - \phi$ and (b) the ASV target-tracking error $\|P_f - P(t)\|$.

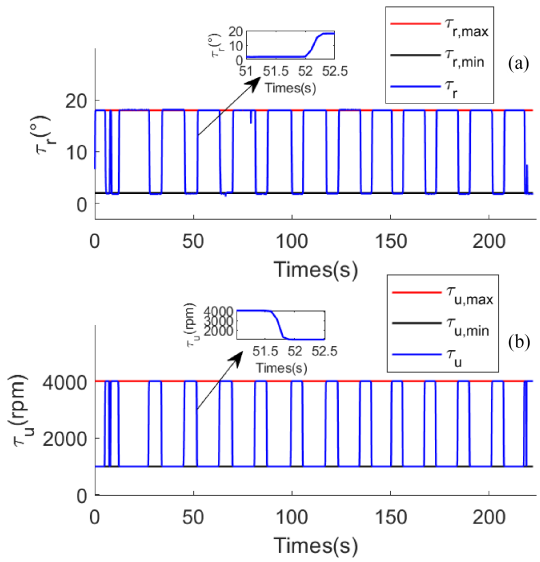

Fig. 9. Temporal behaviors of the ASV control inputs (a) τ_r and (b) τ_u in (11).

$T_s = 100$ ms. During online control law calculation, the solution of ϕ involves historical data of ASV positions and headings. Fortunately, since Algorithm 1 only conducts basic calculations, the solution of ϕ can be finished within 9 ms, whereas the overall calculation of the control law just takes less than 11 ms, which meets the requirements of real-time control of the system. The onboard calculation platform is STM32F407 MCU with 168M Frequency, 1M Flash, and 192K RAM.

The temporal behaviors of the ASV real-time movement direction $\phi(t)$, direction $\phi_p(P_f - P(t))$, and ASV harbor-tracking error $\|P_f - P(t)\|$ are demonstrated in Figs. 7 and 8. It is observed that both the ASV harbor-heading error $\phi_p(P_f - P(t)) - \phi(t)$ and the ASV target-tracking error $P_f - P(t)$ converge to zero, and the ASV eventually returns to the harbor position P_f, and Problem 1 is solved by the proposed FTC law (10), (11), (17). Note that, as shown in Fig. 9, it is observed

that the ASV suffered from steer jamming fault exerted a suitable continuous propulsion τ_u with a proper continuous nozzle direction τ_r along the periodical spiral moving trajectory. From Figs. 6 and 9, one has that regardless of the state of the actuator, the heading of the ASV has been monotonically increasing, so the ASV cannot keep going straight, but can only return to the harbor in a spiral. This phenomenon can explain the influence of actuator fault on the harbor-returning control.

Eventually, the ASV moves along a regular spiral curve, and ψ_t settles to the desired target direction $\phi_p(P_f - P(t))$; $P(t)$ reaches the destination. The effectiveness of the proposed FTC protocol (10), (11), (17) is thus verified. Moreover, the present ASV control experiment environment is calm-rippled (wave height of 0–0.1 m and wind force of 1). By extensive experiments, the developed closed-control ASV system has shown robustness to external disturbances like winds, waves, and currents, which could, thus, be expected to help pave the way from ASV FTC theory to real maritime ASV applications.

VI. Conclusion

Monotonic input constraints induced by steer jamming are often encountered in ASV operations, which inevitably hinders the further applications of ASVs to complex modern maritime operations. To address such a challenge, a PFC law was developed to exert a suitable water jetting propulsion with a proper nozzle angle along with consecutive positions of ASV spiral moving trajectories. Sufficient conditions were derived to guarantee the asymptotical stability of the proposed FTC law for autonomous harbor returning. The effectiveness of the proposed control algorithm was verified via lake-based experiments on a HUSTER-16 ASV platform.

References

[1] B. S. Park and S. J. Yoo, "Robust fault-tolerant tracking with predefined performance for underactuated surface vessels," *Ocean Eng.*, vol. 115, pp. 159–167, 2016.

[2] M. Fu, M. Li, and W. Xie, "Finite-time trajectory tracking fault-tolerant control for surface vessel based on time-varying sliding mode," *IEEE Access*, vol. 6, pp. 2425–2433, 2018.

[3] M. Fu, T. Wang, and C. Wang, "Adaptive neural-based finite-time trajectory tracking control for underactuated marine surface vessels with position error constraint," *IEEE Access*, vol. 7, pp. 16309–16322, 2019.

[4] Y. Lin, J. Du, G. Zhu, and H. Fang, "Thruster fault-tolerant control for dynamic positioning of vessels," *Appl. Ocean Res.*, vol. 80, pp. 118–124, 2018.

[5] Y. Zheng, Z. Liu, and L. Liu, "Robust MPC-based fault-tolerant control for trajectory tracking of surface vessel," *IEEE Access*, vol. 6, pp. 14755–14763, 2018.

[6] X. Hu, J. Du, G. Zhu, and Y. Sun, "Robust adaptive NN control of dynamically positioned vessels under input constraints," *Neurocomputing*, vol. 318, no. 27, pp. 201–212, 2018.

[7] S. He and S. Dai, and F. Luo, "Asymptotic trajectory tracking control with guaranteed transient behavior for MSV with uncertain dynamics and external disturbances," *IEEE Trans. Ind. Electron.*, vol. 66, no. 5, pp. 3712–3720, May 2019.

[8] L. Chen, R. Cui, C. Yang, and W. Yan, "Adaptive neural network control of underactuated surface vessels with guaranteed transient performance: Theory and experimental results," *IEEE Trans. Ind. Electron.*, vol. 67, no. 5, pp. 4024–4035, May 2020.

[9] L. Cavanini and G. Lppoliti, "Fault tolerant model predictive control for an over-actuated vessel," *Ocean Eng.*, vol. 160, no. 15, pp. 1–9, 2018.

[10] Z. Zheng, L. Sun, and L. Xie, "Error-constrained LOS path following of a surface vessel with actuator saturation and faults," *IEEE Trans. Syst., Man, Cybern.: Syst.*, vol. 48, no. 10, pp. 1794–1805, Oct. 2018.

[11] N. Wang, X. Pan, and S. Su, "Finite-time fault-tolerant trajectory tracking control of an autonomous surface vehicle," *J. Franklin Inst.*, vol. 357, no. 16, pp. 11114–11135, 2020.

[12] J. Zhang, S. Yu, and Y. Yan, "Fixed-time velocity-free sliding mode tracking control for marine surface vessels with uncertainties and unknown actuator faults," *Ocean Eng.*, vol. 201, 2020, Art. no. 107107.

[13] J. Zhang and G. Yang, "Fault-tolerant fixed-time trajectory tracking control of autonomous surface vessels with specified accuracy," *IEEE Trans. Ind. Electron.*, vol. 67, no. 6, pp. 4889–4899, Jun. 2020.

[14] R. Singh and B. Bhushan, "Condition monitoring based control using wavelets and machine learning for unmanned surface vehicles," *IEEE Trans. Ind. Electron.*, vol. 68, no. 8, pp. 7464–7473, Aug. 2021.

[15] C. Huang, X. Zhang, and G. Zhang, "Adaptive neural finite-time formation control for multiple underactuated vessels with actuator faults," *Ocean Eng.*, vol. 222, 2021, Art. no. 108556.

[16] J. Ghommam and M. Saad, "Adaptive leader–follower formation control of underactuated surface vessels under asymmetric range and bearing constraints," *IEEE Trans. Veh. Technol.*, vol. 67, no. 2, pp. 852–865, Feb. 2018.

[17] Z. Peng, Y. Jiang, and J. Wang, "Event-triggered dynamic surface control of an underactuated autonomous surface vehicle for target enclosing," *IEEE Trans. Ind. Electron.*, vol. 68, no. 4, pp. 3402–3412, Apr. 2021.

[18] Z. Peng, J. Wang, D. Wang, and Q.-L. Han, "An overview of recent advances in coordinated control of multiple autonomous surface vehicles," *IEEE Trans. Ind. Informat.*, vol. 17, no. 2, pp. 732–745, Feb. 2021.

[19] T. Fossen, *Guidance and Control of Ocean Vehicles*. Chichester, U.K.: Wiley, 1994.

[20] D. Chwa, "Global tracking control of underactuated ships with input and velocity constraints using dynamic surface control method," *IEEE Trans. Control Syst. Technol.*, vol. 19, no. 6, pp. 1357–1370, Nov. 2011.

[21] H. K. Khalil and J. W. Grizzle, *Nonlinear Systems*. Hoboken, NJ, USA: Prentice-Hall, 1996.

[22] B. Liu et al., "Collective dynamics and control for multiple unmanned surface vessels," *IEEE Trans. Control Syst. Technol.*, vol. 28, no. 6, pp. 2540–2547, Nov. 2020.

Bin Liu received the B.S. degree in automation from the Wuhan University of Technology, Wuhan, China, in 2014, and the Ph.D. degree in control science and engineering from the Huazhong University of Science and Technology, Wuhan, in 2019.

He is currently a Postdoctoral Researcher with the Huazhong University of Science and Technology. His research interests include multi-unmanned-surface-vehicle formation control, unmanned surface vessel control, and model-predictive control.

Hai-Tao Zhang (Senior Member, IEEE) received the B.E. degree in automation and the Ph.D. degree in control science and engineering from the University of Science and Technology of China, Hefei, China, in 2000 and 2005, respectively.

From January 2007 to December 2007, he was a Postdoctoral Researcher with the University of Cambridge, Cambridge, U.K. Since 2005, he has been with the Huazhong University of Science and Technology, Wuhan, China, where he was an Associate Professor from 2005 to 2010 and has been a Full Professor since 2010. His research interests include swarming intelligence, model-predictive control, and unmanned system cooperation control.

Dr. Zhang is a recipient of National Science Fund for Distinguished Young Scholars. He is/was an Associate Editor for IEEE Transactions on Systems, Man, and Cybernetics: Systems, IEEE Transactions on Circuits and Systems II: Express Briefs, *Engineering*, and *Asian Journal of Control*.

Haofei Meng received the B.E. degree in process equipment and control engineering from the Wuhan University of Technology, Wuhan, China, in 2010, the M.E. degree in control science and engineering from the University of Science and Technology of China, Hefei, China, in 2013, and the Ph.D. degree in electrical engineering from the University of Newcastle, Callaghan, NSW, Australia, in 2017.

From 2018 to 2020, she was a Postdoctoral Researcher with the Huazhong University of Science and Technology, Wuhan. She is currently an Associate Researcher with Southeast University, Nanjing, China. Her research interests include multiagent systems, time-delay systems, and switched systems.

Jun Wang (Life Fellow, IEEE) received his B.S. degree in electrical engineering and M.S. degree in systems engineering from Dalian University of Technology, Dalian, China, in 1982 and 1985, respectively, and his Ph.D. degree in systems engineering from Case Western Reserve University, Cleveland, OH, USA, in 1991.

He held various academic positions with Dalian University of Technology, Case Western Reserve University, University of North Dakota, Grand Forks, ND, USA, and the Chinese University of Hong Kong, Hong Kong. He also held various short-term or part-time visiting positions with the U.S. Air Force Armstrong Laboratory, Dayton, OH, USA; RIKEN Brain Science Institute, Tokyo, Japan; Huazhong University of Science and Technology, Wuhan, China; Shanghai Jiao Tong University, Shanghai, China; and Dalian University of Technology. He is currently a Chair Professor with City University of Hong Kong, Hong Kong.

Dr. Wang was a recipient of several awards including the Research Excellence Award from the Chinese University of Hong Kong in 2008–2009, the Outstanding Achievement Award from Asia-Pacific Neural Network Assembly in 2011, the IEEE TRANSACTIONS ON NEURAL NETWORKS Outstanding Paper Award in 2011, the Neural Networks Pioneer Award from the IEEE Computational Intelligence Society in 2014, and the Norbert Wiener Award from the IEEE Systems, Man, and Cybernetics Society in 2019. He was the General Chair of the 13th/25th International Conference on Neural Information Processing from 2006 to 2018 and the IEEE World Congress on Computational Intelligence in 2008. He is a Distinguished Lecturer of the IEEE Systems, Man, and Cybernetics Society from 2017 to 2022. He was a Distinguished Lecturer of the IEEE Computational Intelligence Society from 2010 to 2012 and from 2014 to 2016. He was the Editor-in-Chief for IEEE TRANSACTIONS ON CYBERNETICS from 2014 to 2019.